Chemical Science

ROYAL SOCIETY OF CHEMISTRY

EDGE ARTICLE

View Article Online
View Journal

Check for updates

Cite this: DOI: 10.1039/d6sc00603e

All publication charges for this article have been paid for by the Royal Society of Chemistry

Combined electrodeposition and electropolymerization method to produce surface-bound polystyrenyl NHC thin films

Jessica L. Bosso,[ab] Justin T. Lomax,[ab] Garima Garg,[ab] Wai-Tung Shiu,[ab] Jordan N. Bentley,[ab] Matthew J. Turnbull,[ab] Monika R. Snowdon,[bc] James J. Noël,[*abd] Cathleen M. Crudden,[*bc] Joe B. Gilroy[*ab] and Paul J. Ragogna[*abd]

Polymeric *N*-heterocyclic carbene (NHC) films offer a promising strategy for generating durable protective coatings on metals. Polystyrenyl NHC films were constructed on gold in a one step process that combined electrodeposition and electropolymerization of styrenyl benzimidazolium halide precursors at −1.3 V *vs.* Ag/AgCl for 5 min. Ellipsometry confirmed the nanometer scale films on Au were formed with thicknesses of 1.2–2.9 ± 0.2 nm, while non-polymerizable controls were ≤0.8 nm. Cyclic voltammetry showed strong surface passivation for all polystyrenyl NHC films relative to the monomeric analogues. Area selective deposition on the NHC precursors was evaluated on patterned Au/SiO_2 with excellent selectivity factors up to 0.90. These results establish polystyrenyl NHC films as robust nanometer-thick inhibitor coatings that couple strong NHC–metal bonding with the hydrophobic insulating character of polystyrene.

Received 21st January 2026
Accepted 9th March 2026

DOI: 10.1039/d6sc00603e

rsc.li/chemical-science

Open Access Article. Published on 10 March 2026. Downloaded on 4/21/2026 2:30:29 PM.
This article is licensed under a Creative Commons Attribution-NonCommercial 3.0 Unported Licence.

Introduction

Corrosion remains a major industrial burden, costing an estimated 2.5 trillion USD each year, equating to ∼3.4% of the world's gross domestic product.[1] The oil and gas,[2] automotive,[3] aerospace,[4] energy,[5] and maritime[6] industries are significantly impacted by corrosion, as each requires large-scale metal infrastructure that is susceptible to degradation. The cost of corrosion could be reduced by 15–35% through the use of effective anti-corrosion methods (*e.g.*, barrier coatings),[7,8] electrochemical polarization (*e.g.*, anodic and cathodic protection)[9–11] and proper material design (*e.g.*, Al-based amorphous alloys).[12–14] Among these approaches, polymeric coatings are widely used because they are inert, inexpensive, and mechanically robust.[15] Polystyrene in particular has shown significant value in extending the lifetime and corrosion resistance of protective films.[16,17] Although useful for corrosion protection, polymeric barriers suffer from weak adhesion to metal substrates due to their low surface energy (*e.g.*, polystyrene = 36–42 mJ m^{-2}) and absence of anchoring groups. External factors, such as molecular weight, surface treatments and temperature, can further amplify this weakness.[18–21] The lack of polar functional groups that could anchor the main chain to the substrate is a key contributor to poor adhesion properties.[22] These limitations highlight the need for films that form stronger, more chemically robust linkages with the metal surface. Self-assembled monolayers (SAMs) are known for the formation of dense films on metal surfaces through chemisorptive interactions.[23,24] While many SAMs are based on thiols, these have issues of oxidative and thermal instability. *N*-Heterocyclic carbenes (NHCs), by comparison, have emerged as particularly powerful surface ligands, offering exceptional binding strength and high chemical and thermal stability.[25–31] A variety of routes can be employed to generate SAMs from NHC precursors which are generally formed *via* immersion of a metal substrate into a solution containing the surface ligand precursor.[26,32] In most cases, deprotonation of a charged NHC precursor such as an imidazolium derivative needs to take place prior to reaction and assembly onto the metal surface.[33,34]

Electrochemical deposition (or electrodeposition) is a useful method for NHC SAM formation that is proposed to generate the NHCs through the formation of hydroxide ions produced *via* water electroreduction.[35] In the case of wingtip-functionalized alkynyl NHC precursors, the application of electrodeposition conditions led to simultaneous polymerization of the unsaturated wingtip groups, forming a poly(NHC) nanolayer.[36] The polymeric NHC film exhibited anti-corrosion properties on copper substrates, as well as high thermal and chemical

[a]*Department of Chemistry, University of Western Ontario, London, ON, N6A 3K7, Canada. E-mail: pragogna@uwo.ca*

[b]*Carbon to Metal Coating Institute, Queen's University, Kingston, ON, K7L 3N6, Canada*

[c]*Department of Chemistry, Queen's University, 90 Bader Lane, Kingston, ON, K7L 3N6, Canada*

[d]*Surface Science Western, 999 Collip Cir, London, ON, N6G 0J3, Canada*

Open Access Article. Published on 10 March 2026. Downloaded on 4/21/2026 2:30:29 PM.
This article is licensed under a Creative Commons Attribution-NonCommercial 3.0 Unported Licence.

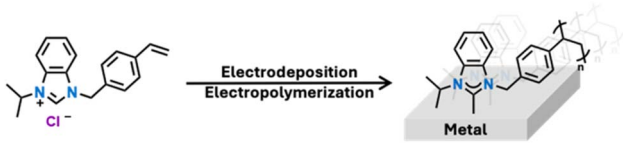

Fig. 1 Simultaneous electrodeposition and electropolymerization of styrenyl-bearing imidazolium salts for the formation of polystyrenyl NHCs bound to metal surfaces.

stability. Based on these observations, polymeric NHC-based surface coatings were hypothesized to have strong interfacial bond energies and mitigate metal degradation.[36] Considering the well-known ability of polystyrene-type polymers to act as protective films, we undertook a study of polystyrene-functionalized NHCs to determine whether they could be electropolymerized onto metal surfaces, and whether the resulting coatings would provide improved protection to the underlying surface. This approach leverages decades of research into polystyrene-type polymers, including a well-defined polymerization mechanism that is known to be base-initiated, and our groups' knowledge of NHC chemistry.[25,37–39]

Herein, we describe the electrodeposition and electropolymerization of styrenyl imidazolium precursors to generate polystyrenyl NHCs on gold surfaces (Fig. 1). This one-step process generates strongly bound, polymeric coatings that combine the stability of NHC–metal linkages with the hydrophobic, insulating properties of polystyrene. The resulting films display enhanced electrochemical passivation and stability relative to monomeric analogues and can be patterned with area selectivity.

Results and discussion

We began by preparing benzimidazolium derivatives in which two (**1-Cl**) or one (**2-Cl**) wingtip contains a polymerizable styrene to enable the synthesis of linear polymer chains and cross-linked networks. Styrene units were introduced *via* *N*-alkylation of benzimidazole with the corresponding benzyl halides (Fig. 2a). ^{1}H NMR spectra of the benzimidazolium chloride salts (Fig. S3 & S5) showed a resonance at approximately $\delta = 10$ ppm, indicating the successful quaternization of benzimidazole to form the corresponding salt. Radical polymerization of **2-Cl** in solution using azobisisobutyronitrile (AIBN) as the initiator enabled the synthesis of polystyrenyl NHC precursor **3-Cl**, which serve as a comparison to on-surface polymerization (Fig. 2b). The ^{1}H NMR spectra of **2-Cl** and **3-Cl** (Fig. S4 & S5) revealed broadened signals and consumption of styrene based on the reduction of the intensity of the vinyl signals, indicative of a successful oligo/polymerization of **2-Cl**.

The determination of the molecular weight (MW) of the solution-prepared polymer **3-Cl** was attempted using gel permeation chromatography (GPC); however, the ionic nature of the polymer precluded this measurement on our systems. Diffusion-ordered spectroscopy (DOSY) was instead employed to estimate the MW of **3-Cl**, as DOSY has been established as an effective method for determining the MW of polymers.[40–42] The

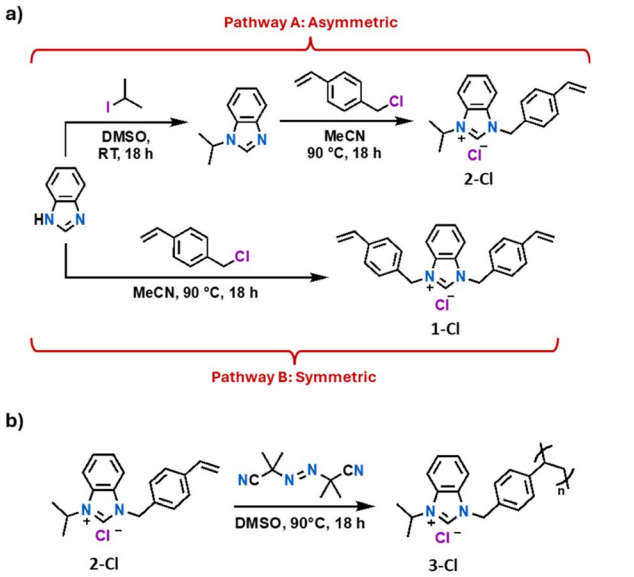

Fig. 2 (a) Synthetic pathways towards **2-Cl** (Pathway A) and **1-Cl** (Pathway B) styrenyl benzimidazolium chloride salts. (b) Free radical polymerization of **2-Cl** with AIBN as the radical initiator.

logarithm of the diffusion coefficient (D) of **3-Cl** was determined and the molecular weight (MW) of the sample was estimated from the line of best fit of the log(D) *vs.* log(M) plot from the calibration curves obtained from poly(ethylene glycol) and polystyrene standards (Fig. S1 and S2). Based on the DOSY analysis relative to the PEG and PS standards, the molecular weight of **3-Cl** was calculated to be approximately 30 000 g mol^{-1}, confirming the effective polymerization of **2-Cl**.

Having established the molecular structures and polymerization behaviour of styrenyl precursors in solution, we next performed the electrodeposition of styrenyl NHCs **1-Cl** and **2-Cl**. Our aim is to construct dense films on the surface by simultaneously achieving NHC deposition and styrene electropolymerization, which proceeds at negative potentials (Fig. 3a).[35,43] Au substrates were used as working electrodes after rigorous cleaning protocols (see SI). Solutions of the desired NHC precursors were placed in a deposition solution containing a nBu$_4$NPF$_6$ (0.1 M), triple-distilled water (55 mM) with DMSO as solvent, which was sparged with N$_2$ for 30 min after mixing. The working electrodes were then immersed in the deposition solution under a flow of Ar, and a constant potential of −1.3 V *vs.* a Ag/AgCl ([Cl$^-$] = 1 M reference electrode) was applied for 5 min.[44] The electrodes were rinsed with copious amounts of DMSO, water, and then MeOH after deposition to remove residual precursor from the surfaces. As a comparison, **3-Au** was prepared by the electrodeposition of the pre-polymerized solution of **3-Cl** (20 mM) under identical conditions (−1.3 V *vs.* Ag/AgCl for 5 min). The polymer control enabled the direct comparison of films formed *via* on-surface electropolymerization *versus* the deposition of pre-synthesized polymeric species. Although conditions were held constant here to enable direct comparison, film thickness in

© 2026 The Author(s). Published by the Royal Society of Chemistry

Open Access Article. Published on 10 March 2026. Downloaded on 4/21/2026 2:30:29 PM.
This article is licensed under a Creative Commons Attribution-NonCommercial 3.0 Unported Licence.

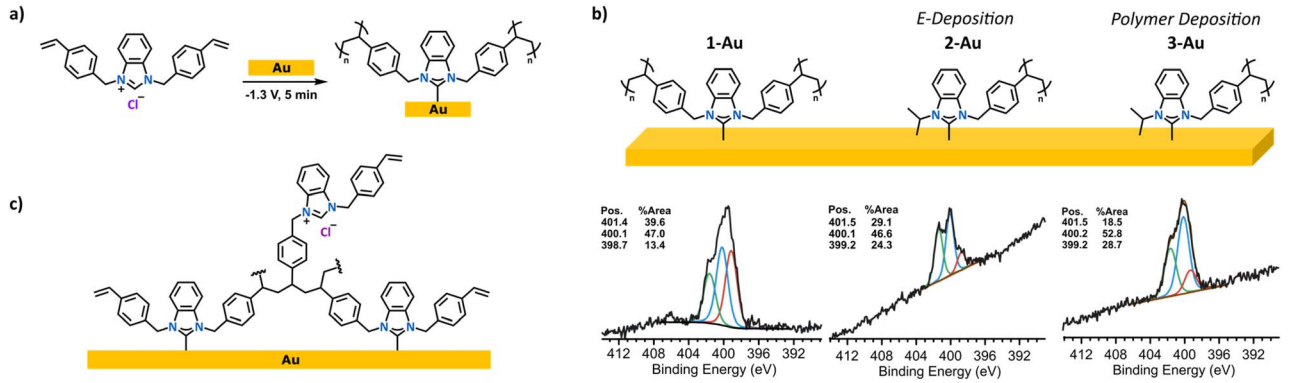

Fig. 3 (a) Electrochemical deposition of imidazolium chloride salt **1-Cl** onto a Au electrode. (b) High-resolution N 1s XPS spectra collected for electrodeposited films of **1-Au**, **2-Au**, and **3-Au**, showing the emergence of surface-bound NHC. (c) Illustration of the incorporation of unreacted imidazolium salt in the growing polymer network during electrochemical deposition.

electrochemical deposition can be tuned by adjusting parameters such as potential, time, and precursor concentration.[36]

Time-of-flight secondary ion mass spectrometry (ToF-SIMS) analysis of surface-bound films **2-Au** and **3-Au** (Fig. S14 and S15) showed fragmentation patterns attributed to the polystyrenyl wingtip (104 *m*/*z*) and the molecular ion of the parent precursor, confirming the formation of NHC coatings. The low intensity of the signals was attributed to high fragmentation from the nature of ToF-SIMS.[45–47] Signals corresponding to a styrenyl fragment (117 *m*/*z*) and benzimidazole core (119 *m*/*z*) were evident in the spectra and also confirmed NHC-functionalization of the surface.

The observation of a monomeric molecular ion signal in **3-Au** suggested that residual monomer was present in the deposited polymer. The spectrum of **1-Au** (Fig. S13) did not exhibit the molecular ion signal, suggesting that in this case, the majority of monomeric species were consumed during the on-surface polymerization process.

Having identified conditions under which polymerization could be affected on the surface, we next probed whether NHC polymers were physi- or chemisorbed. X-ray photoelectron spectroscopy (XPS) was employed to monitor the binding energy (BE) shift from imidazolium salt to surface bound species (Fig. 3b). Previous reports have shown that surface bound NHCs have N 1s signals at *ca.* 400.2 eV,[44,48–51] while the starting benzimidazolium salts appear at *ca.* 401.5 eV. Polymer-bound NHC polymers **1-Au** and **2-Au** have a major signal at 400.1 eV, indicating that polymer binding to the surface occurs by chemisorption. An additional signal at 401.4 eV is observed and ascribed to trapped ammonium from the electrolyte or unreacted imidazolium precursors (Fig. S18 & S19).

To assess whether the signal at 401.5 eV arose from polymer-trapped precursor or electrolyte rather than simple physisorption, we prepared control samples with **4-Br** and **5-Br**, which are the non-polymerizable structural analogues of **1-Cl** and **2-Cl** (Fig. 4). These benzyl salts were subjected to the same electrodeposition and washing steps as above. The N 1s XPS spectra of **4-Au** and **5-Au** displayed an intense monomodal peak centred at 400.2 eV, indicative of a surface-bound NHC and a negligible amount of precursor (Fig. 4). The effective removal of benzyl salts *via* washing provided evidence for styrene polymerization as the benzyl precursors were not bound in a polymer. From these observations, we attribute the signal at 399 eV to correspond to reduced electrolyte at the surface and/or other N organic species of the polymerized NHC surfaces.[49,52,53] Since the electroreduction of styrene occurs at negative potentials through an irreversible process and in polar aprotic solvents,[43,54–57] the application of a potential of −1.3 V *vs.* Ag/AgCl during electrodeposition is sufficient to initiate polymerization in the absence of an external initiator. An alternative possibility, however, involves the initiation of a radical polymerization by butyl radicals derived from the ammonium-based electrolyte. These radical species could have initiated the styrene monomer at the surface and set off a free radical polymerization pathway. The existence of butyl radicals was supported by evidence of amines in the N 1s XPS spectrum of **2-Au** on gold since the mechanism for tertiary amine generation involves generation of a butyl radical.[52,53] A third plausible pathway is the electroreduction of the quaternary ammonium electrolyte, producing a tertiary amine that then deprotonates the monomer and initiates polymerization.[39,57] It is also possible that all three mechanisms are simultaneously in play, as all are possible under the experimental conditions employed.

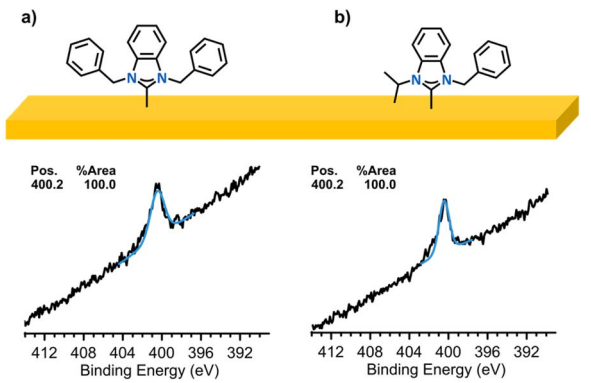

Fig. 4 High-resolution N 1s XPS spectra of (a) **4-Au** and (b) **5-Au** after electrodeposition and washing.

Open Access Article. Published on 10 March 2026. Downloaded on 4/21/2026 2:30:29 PM. This article is licensed under a Creative Commons Attribution-NonCommercial 3.0 Unported Licence.

Ellipsometry measurements of the films provided additional evidence for electropolymerization of compounds **1-Cl** and **2-Cl**. Films **1-Au**, **2-Au**, and **3-Au** were measured to be 2.9 ± 0.2 nm, 1.2 ± 0.1 nm, and 2.9 ± 0.2 nm thick, respectively, whereas films **4-Au** and **5-Au** were only 0.8 and ∼0 nm, respectively. The thickness of the NHC films suggest that, indeed, multiple layers were formed on the Au electrodes, likely arising to several layers of "trapped" imidazolium salts crosslinked in the growing polymer.

Roughness was constant among all samples, and therefore, differences in measured thickness were attributed to NHC film growth. The nanometer-scale thicknesses observed for **1-Au** and **3-Au** suggest the formation of multilayered polymeric structures rather than simple monolayers, likely arising from crosslinked or overlapping polymer domains formed during electrodeposition. Reports of electropolymerized alkynyl-NHC nanolayers indicate a thicknesses of approximately 2.0 ± 0.5 nm,[36] which similarly correspond to stacked or crosslinked NHC assemblies.

Cyclic voltammetry (CV) was used to probe the surface passivation properties of the styrenyl NHC films. Cyclic voltammograms of bare and functionalized Au electrodes were recorded in an aqueous solution of ferri/ferrocyanide, so that inhibition of electron transfer to the redox active iron center by the insulating polymer film on the surface could be probed. Bare gold electrodes were expected to produce a classic "duck-shaped" trace, resulting from the redox of ferri/ferrocyanide from solution. By comparison, NHC-functionalized surfaces would exhibit a more flattened shape as the NHC layer prevents the solution species from reaching the metal surface to undergo redox.[48] CV traces of Au electrodes functionalized with **1-Au**, **2-Au**, and **3-Au** (Fig. 5a–c) showed nearly complete suppression of current passage. The strong blocking observed provides additional evidence for on-surface electropolymerization of styrene, since simple unpolymerized NHC-SAMS **4-Au** and **5-Au** passivate the surface to a much lower extent[58] (Fig. 5d and e). The CV data also provided insight into the differing performance of cross-linked and linear polymer films. Films of **1-Au** exhibited better passivation than those of **2-Au**, likely attributed to the increased cross-linking of this film provided by the presence of two styrene units. The CV of **2-Au** showed only cathodic current, and this arose only at potentials below ∼100 mV *vs.* Ag/AgCl, suggesting that the film blocked ferri/ferrocyanide redox but still permitted the reduction of dissolved oxygen from the solution.

Electrochemical impedance spectroscopy (EIS) was used to determine the charge transfer resistance (R_{ct}) of the poly-NHC films, with higher resistance values translating to better protection of the surface.[59] Nyquist plots collected for **1-Au**-, **2-**

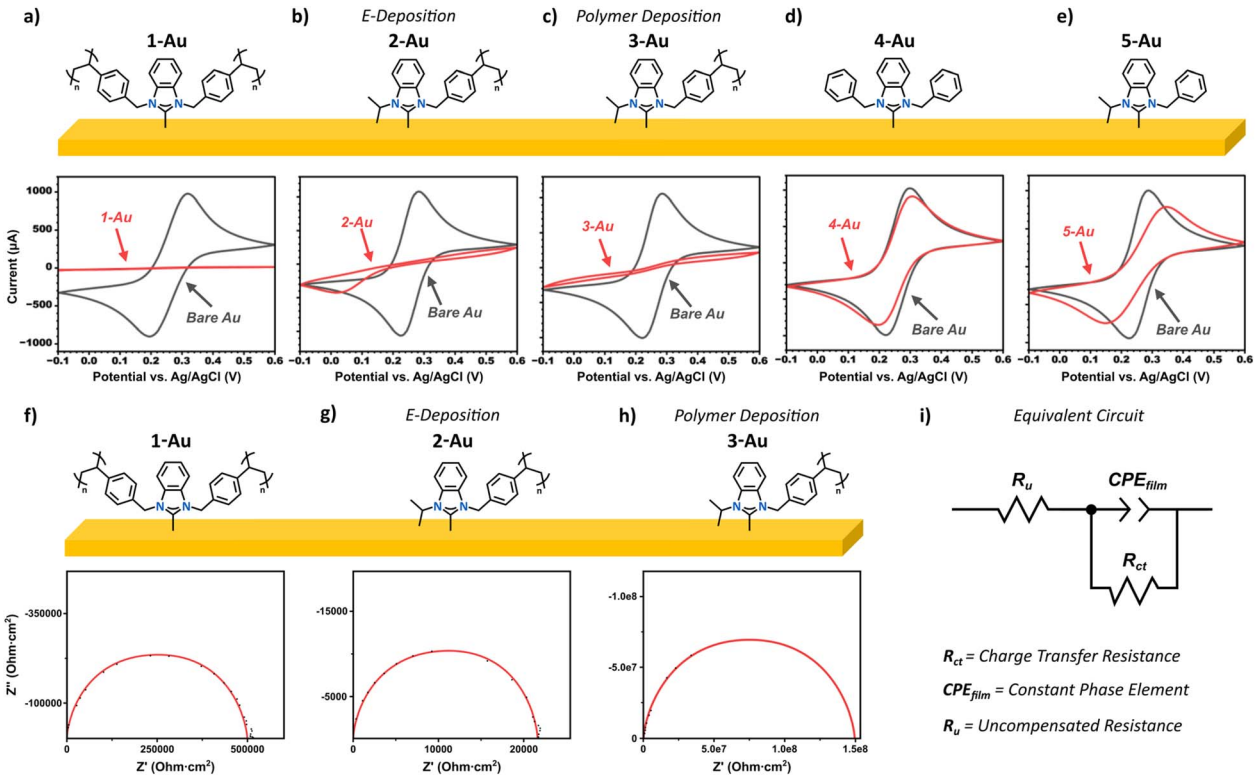

Fig. 5 Electrochemical characterization of polystyrenyl NHC films on gold. Schematic representations of the NHC-modified electrodes are shown above each panel. (Top) Cyclic voltammograms of bare Au (grey) and Au modified with (a) **1-Au**, (b) **2-Au** (c) **3-Au** (d) **4-Au** and (e) **5-Au** recorded in an aqueous ferri/ferrocyanide solution, with strong suppression of current for the polystyrenyl NHC films compared to the non-polymerizable controls. (Bottom) Nyquist plots of (f) **1-Au**, (g) **2-Au**, and (h) **3-Au**-functionalized gold surface. The equivalent circuit model used to fit the EIS data is shown in (i); R_u is the uncompensated (solution) resistance, R_{ct} the charge transfer resistance, and CPE_{film} the constant phase element representing the slightly non-ideal capacitance of the deposited film on the electrode surface.

© 2026 The Author(s). Published by the Royal Society of Chemistry

Open Access Article. Published on 10 March 2026. Downloaded on 4/21/2026 2:30:29 PM.
This article is licensed under a Creative Commons Attribution-NonCommercial 3.0 Unported Licence.

Au-, and **3-Au**-functionalized gold surfaces (Fig. 5f–h) were fitted using the equivalent circuit, yielding R_{ct} values of 499 kΩ cm^{-2}, 21.6 kΩ cm^{-2}, and 149 MΩ cm^{-2}, respectively. The fitted models are shown with the data in Fig. 5f–h.

All three films exhibited effective blocking behaviour, with the **3-Au** film besting the other two by nearly 3 orders of magnitude. This is increase in performance is attributed to the higher molecular weight of the pre-synthesized polymer (30 000 g mol^{-1}). While the electropolymerized films are limited by surface constraints during growth, the pre-formed polymer deposits as a cohesive, overlapping barrier that more effectively minimizes pinholes and ion permeation. These Nyquist plots lacked the 45° line characteristic of Warburg behaviour, which indicated that even at low frequencies the redox response within the NHC coating was not governed by diffusion. The constant phase element (CPE) parameter values were in the range of 1 ± 0.2 μF^{n}•cm^{-2} in each case, where $1 > n > 0.95$ in each case, consistent with a thin interfacial film with a low dielectric constant and slightly non-ideal capacitive behaviour. Cross-linked polymeric film **1-Au** exhibited improved R_{ct} compared to **2-Au**. This interpretation is consistent with the CV results. In addition to possible applications in corrosion resistance, NHC polymer films may also have applications in semiconductor microchip manufacturing. The selective deposition of monomeric NHCs on metals co-located with dielectric regions (*e.g.*, silicon dioxide) has been demonstrated by our groups to occur with high precision.[50] Area-selective electrodeposition of NHCs was demonstrated by Gross and co-workers, who formed nitro- and fluorine-functionalized NHC SAMs on Au microelectrode arrays.[44] Considering these two precedents, we examined the possibility of area-selective electrodeposition to form polymeric NHCs enabling increased stability and surface density.

To assess the feasibility of polymeric NHC area-selective deposition, polystyrenyl NHCs **1-Cl** and **2-Cl** were electrodeposited on gold and silicon dioxide patterned substrates having alternating 100 μm bands of metal and dielectric. Patterned wafers were immersed in a deposition solution containing 20 mM styrenyl NHC precursor, electrolyte, and DMSO, and simultaneous electrodeposition and electropolymerization were performed as previously described. ToF-SIMS mapping experiments were carried out on substrates functionalized with **1-Au**, **2-Au**, and **3-Au** to visualize the spatial distributions of various fragments. Samples were scanned for the mass/charge ratio of Si^{+} to determine the location of silicon dioxide bands on the surface (Fig. 6a–c). The mass of a methyl benzene cation ($C_7H_7^{+}$), a polystyrene fragment, was targeted as evidence of NHC deposition, since polystyrenyl NHCs readily fragment. ToF-SIMS images prepared highlighting the location of this styrene fragment (Fig. 6d–f) exhibited brighter areas in the gold regions, detailing that the styrene fragment was produced primarily on the metal bands. The mapped ToF-SIMS spectra scanning for each styrenyl ion fragment of the NHCs (Fig. 6g–i) yielded selectivity factors of up to 0.90, confirming preferential deposition on Au bands. The lesser contrast between Au and dielectric regions in the molecular ion of a single monomer of the data was likely a result of the polystyrenyl NHC fragmentation, as the amount detected on the gold bands was inherently lower. This is the first example of the one-step, area-selective electrodeposition and electropolymerization of NHCs, and has potential as a new polymeric surface inhibitor process in nanofabrication.[18]

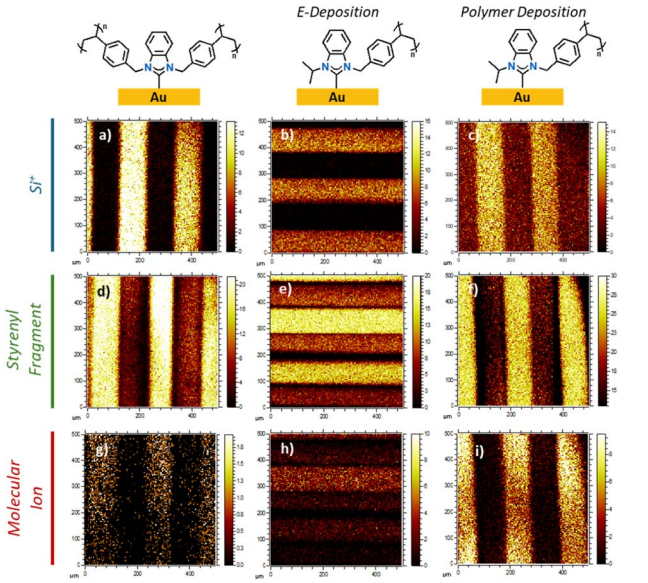

Fig. 6 (Top) ToF-SIMS image scanned for Si^{+} (28 *m*/*z*) on (a) **1-Au**, (b) **2-Au**, and (c) **3-Au**-functionalized patterned wafer. (Middle) ToF-SIMS image scanned for a styrenyl fragment (91 *m*/*z*) on (d) **1-Au**, (e) **2-Au**, and (f) **3-Au**-functionalized patterned wafer. (Bottom) ToF-SIMS image scanned for the molecular ion (351 *m*/*z*) on (g) **1-Au**, (h) **2-Au**, and (i) **3-Au**-functionalized patterned wafer.

Conclusions

Polystyrenyl NHC films on gold surfaces were formed in a one-step, simultaneous electrodeposition and electropolymerization process. These films contained precursor salts that were not removed *via* washing, which were hypothesized to be incorporated into the surface-bound polymer. Control experiments using NHCs without polymerizable groups support this conclusion, as these non-polymerizable derivatives did not contain substantial residual precursor after washing. The polymeric NHC coating **3-Au** had excellent surface passivation properties, inhibiting the passage of current when analyzed using CV. It was also shown that the cross-linked film, **1-Au**, performed better at metal passivation than the linear polymer, **2-Au**, likely due to increased density and stability. Nyquist plots of the polystyrenyl NHCs showed that **1-Au** exhibited higher R_{ct} than **2-Au**, supporting the claim that the cross-linked film passivated the surface more than the linear polymer. The pre-formed polymer film displayed the highest R_{ct} value. While gold was employed here as a model substrate, the electrochemical deposition strategy described in this work is expected to be compatible with other conductive metal surfaces. ToF-SIMS mapping experiments were performed to demonstrate the first example of a one-step, area-selective electrodeposition

Open Access Article. Published on 10 March 2026. Downloaded on 4/21/2026 2:30:29 PM. This article is licensed under a Creative Commons Attribution-NonCommercial 3.0 Unported Licence.

and electropolymerization process of NHCs; a potential new class of inhibitor materials for nanofabrication.

Author contributions

The manuscript was written through contributions of all authors. All authors have given approval to the final version of the manuscript.

Conflicts of interest

There are no conflicts to declare.

Data availability

Supplementary information (SI): synthetic and electrodeposition procedures; NMR, ToF-SIMS, XPS, CV, EIS, and chronoamperometry data. See DOI: https://doi.org/10.1039/d6sc00603e.

Acknowledgements

The authors would like to thank the Natural Sciences and Engineering Council of Canada (NSERC), the Canada Foundation for Innovation (CFI), the New Frontiers in Research Fund (NFRF), Surface Science Western (SSW), the Western Nanofabrication Facility, and the Carbon to Metal Coating Institute (C2MCI) at Queen's University for their support.

Notes and references

1 H. Kania, *Coatings*, 2023, **13**, 216.
2 T. E. Perez, *JOM*, 2013, **65**, 1033–1042.
3 A. Chami, R. Benabbou, M. Taleb, Z. Rais and M. El haji, *Mater. Today Proc.*, 2021, **45**, 7636–7642.
4 E. Herzberg, in *Corrosion Control in the Aerospace Industry*, ed. S. Benavides, Woodhead Publishing, 2009, pp. 17–34.
5 F. Cattant, D. Crusset and D. Féron, *Mater. Today*, 2008, **11**, 32–37.
6 B. Valdez, J. Ramirez, A. Eliezer, M. Schorr, R. Ramos and R. Salinas, *J. Mar. Eng. Technol.*, 2016, **15**, 124–134.
7 M. Fenker, M. Balzer and H. Kappl, *Surf. Coat. Technol.*, 2014, **257**, 182–205.
8 G. Kordas, *Corros. Mater. Degrad.*, 2022, **3**, 376–413.
9 C. Edeleanu, *Platin. Met. Rev.*, 1960, **4**, 86–91.
10 P. Pedeferri, *Constr. Build. Mater.*, 1996, **10**, 391–402.
11 R. Juchniewicz, J. Jankowski and K. Darowicki, in *Materials Science and Technology: A Comprehensive Treatment*, John Wiley & Sons, Ltd, 2000, pp. 383–470.
12 L. M. Zhang, S. D. Zhang, A. L. Ma, H. X. Hu, Y. G. Zheng, B. J. Yang and J. Q. Wang, *Corros. Sci.*, 2018, **144**, 172–183.
13 T. Peng, R. Xiao, Z. Rong, H. Liu, Q. Hu, S. Wang, X. Li and J. Zhang, *Chem.–Asian J.*, 2020, **15**, 3915–3941.
14 N. Haridharan and R. V. Shiva Kumar, in *Novel Anti-Corrosion and Anti-Fouling Coatings and Thin Films*, John Wiley & Sons, Ltd, 2024, pp. 353–398.
15 S. Chen, X. Li, Y. Li and J. Sun, *ACS Nano*, 2015, **9**, 4070–4076.
16 L. Románszki, I. Datsenko, Z. May, J. Telegdi, L. Nyikos and W. Sand, *Bioelectrochemistry*, 2014, **97**, 7–14.
17 H. Deveci, G. Ahmetli, M. Ersoz and R. Kurbanli, *Prog. Org. Coat.*, 2012, **73**, 1–7.
18 L. Amar, R. Mondal, O. Blumen, L. Rekanati, I. Berg, S. Harpaz, D. Sharon and E. Gross, *Angew. Chem., Int. Ed.*, 2025, **64**, e202422879.
19 M. Murase and D. Nakamura, *Langmuir*, 2023, **39**, 10475–10484.
20 H. Park, C. B. Park, C. Tzoganakis and P. Chen, *Ind. Eng. Chem. Res.*, 2007, **46**, 3849–3851.
21 J. Hopken and M. Moller, *Macromolecules*, 1992, **25**, 1461–1467.
22 F. Awaja, M. Gilbert, G. Kelly, B. Fox and P. J. Pigram, *Prog. Polym. Sci.*, 2009, **34**, 948–968.
23 Y. Min, M. Akbulut, K. Kristiansen, Y. Golan and J. Israelachvili, *Nat. Mater.*, 2008, **7**, 527–538.
24 N. C. Seeman, *Nature*, 2003, **421**, 427–431.
25 M. N. Hopkinson, C. Richter, M. Schedler and F. Glorius, *Nature*, 2014, **510**, 485–496.
26 C. M. Crudden, J. H. Horton, I. I. Ebralidze, O. V. Zenkina, A. B. McLean, B. Drevniok, Z. She, H.-B. Kraatz, N. J. Mosey, T. Seki, E. C. Keske, J. D. Leake, A. Rousina-Webb and G. Wu, *Nat. Chem.*, 2014, **6**, 409–414.
27 E. Angove, F. Grillo, H. A. Früchtl, A. J. Veinot, I. Singh, J. H. Horton, C. M. Crudden and C. J. Baddeley, *J. Phys. Chem. Lett.*, 2022, **13**, 2051–2056.
28 I. Berg, E. Amit, L. Hale, F. D. Toste and E. Gross, *Angew. Chem., Int. Ed.*, 2022, **61**, e202201093.
29 L. Amar, R. Mondal, O. Blumen, L. Rekanati, I. Berg, S. Harpaz, D. Sharon and E. Gross, *Angew. Chem., Int. Ed.*, 2025, **64**, e202422879.
30 A. Bakker, A. Timmer, E. Kolodzeiski, M. Freitag, H. Y. Gao, H. Mönig, S. Amirjalayer, F. Glorius and H. Fuchs, *J. Am. Chem. Soc.*, 2018, **140**, 11889–11892.
31 C. Vericat, M. E. Vela, G. Benitez, P. Carro and R. C. Salvarezza, *Chem. Soc. Rev.*, 2010, **39**, 1805–1834.
32 A. Chandran, N. L. Dominique, G. Kaur, V. Clark, P. Nalaoh, L. C. Ekowo, I. M. Jensen, M. D. Aloisio, C. M. Crudden, N. Arroyo-Currás, D. M. Jenkins and J. P. Camden, *Nanoscale*, 2025, **17**, 5413–5428.
33 P. de Frémont, N. Marion and S. P. Nolan, *Coord. Chem. Rev.*, 2009, **253**, 862–892.
34 A. V. Zhukhovitskiy, M. G. Mavros, T. Van Voorhis and J. A. Johnson, *J. Am. Chem. Soc.*, 2013, **135**, 7418–7421.
35 E. Amit, L. Dery, S. Dery, S. Kim, A. Roy, Q. Hu, V. Gutkin, H. Eisenberg, T. Stein, D. Mandler, F. Dean Toste and E. Gross, *Nat. Commun.*, 2020, **11**, 5714.
36 I. Berg, E. Amit, L. Hale, F. D. Toste and E. Gross, *Angew. Chem., Int. Ed.*, 2022, **61**, e202201093.
37 J. J. Sanderson and C. R. Hauser, *J. Am. Chem. Soc.*, 1949, **71**, 1595–1596.
38 C. A. Smith, M. R. Narouz, P. A. Lummis, I. Singh, A. Nazemi, C.-H. Li and C. M. Crudden, *Chem. Rev.*, 2019, **119**, 4986–5056.
39 J. D. B. Smith, D. C. Phillips and D. H. Davies, *J. Polym. Sci., Polym. Chem. Ed.*, 1977, **15**, 1555–1562.

© 2026 The Author(s). Published by the Royal Society of Chemistry

Open Access Article. Published on 10 March 2026. Downloaded on 4/21/2026 2:30:29 PM.
This article is licensed under a Creative Commons Attribution-NonCommercial 3.0 Unported Licence.

40 W. Li, H. Chung, C. Daeffler, J. A. Johnson and R. H. Grubbs, *Macromolecules*, 2012, **45**, 9595–9603.
41 P.-J. Voorter, A. McKay, J. Dai, O. Paravagna, N. R. Cameron and T. Junkers, *Angew. Chem., Int. Ed.*, 2022, **61**, e202114536.
42 A. Hu, A. Nyayachavadi, M. Weires, G. Garg, S. Wang and S. Rondeau-Gagné, *RSC Appl. Polym.*, 2023, **1**, 292–303.
43 J. M. Ortega, S. Menolasina, O. P. de Márquez and J. Márquez, *Polymer*, 1986, **27**, 1304–1306.
44 E. Amit, I. Berg, W. Zhang, R. Mondal, H. Shema, V. Gutkin, T. Kravchuk, F. D. Toste, Z. Nairoukh and E. Gross, *Small*, 2024, **20**, 2302317.
45 S. L. Luxembourg and R. M. A. Heeren, *Int. J. Mass Spectrom.*, 2006, **253**, 181–192.
46 M. Körsgen, B. J. Tyler, A. Pelster, D. Lipinsky, K. Dreisewerd and H. F. Arlinghaus, *Biointerphases*, 2016, **11**, 02A318.
47 R. Shishido, M. Fujii, T. Seki, T. Aoki, J. Matsuo and S. Suzuki, *Rapid Commun. Mass Spectrom.*, 2016, **30**, 476–482.
48 C. M. Crudden, J. H. Horton, M. R. Narouz, Z. Li, C. A. Smith, K. Munro, C. J. Baddeley, C. R. Larrea, B. Drevniok, B. Thanabalasingam, A. B. McLean, O. V. Zenkina, I. I. Ebralidze, Z. She, H.-B. Kraatz, N. J. Mosey, L. N. Saunders and A. Yagi, *Nat. Commun.*, 2016, **7**, 12654.
49 A. Nezamzadeh, E. Kaur, M. D. Aloisio, D. A. R. Nanan, Y. S. Hedberg, C. M. Crudden and M. C. Biesinger, *J. Phys. Chem. C*, 2025, **129**, 14177–14189.
50 J. T. Lomax, E. Goodwin, M. D. Aloisio, A. J. Veinot, I. Singh, W.-T. Shiu, M. Bakiro, J. Bentley, J. F. DeJesus, P. G. Gordon, L. Liu, S. T. Barry, C. M. Crudden and P. J. Ragogna, *Chem. Mater.*, 2024, **36**, 5500–5507.
51 V. Singh, T. M. Suduwella, A. Messina, A. Juneau, M. D. Aloisio, C. M. Crudden and J. Mauzeroll, *J. Mater. Chem. A*, 2025, **13**, 37604–37613.
52 A. Adenier, M. M. Chehimi, I. Gallardo, J. Pinson and N. Vilà, *Langmuir*, 2004, **20**, 8243–8253.
53 D. Aurbach and H. Gottlieb, *Electrochim. Acta*, 1989, **34**, 141–156.
54 S. Gambino, A. Gennaro, G. Filardo, G. Silvestri and E. Vianello, *J. Electrochem. Soc.*, 1987, **134**, 2172.
55 P. G. Grodzka and P. J. Elving, *J. Electrochem. Soc.*, 1963, **110**, 231.
56 P. Piotrowski, J. Pawłowska, J. Pawłowski, A. M. Czerwonka, R. Bilewicz and A. Kaim, *RSC Adv.*, 2015, **5**, 86771–86778.
57 B. L. Funt and T. J. Blain, *J. Polym. Sci., Part A-1*, 1970, **8**, 3339–3348.
58 M. Braglia, I. V. Ferrari, T. Djenizian, S. Kaciulis, P. Soltani, M. L. Di Vona and P. Knauth, *ACS Appl. Mater. Interfaces*, 2017, **9**, 22902–22910.
59 C. Chen, *Solids*, 2023, **4**, 254–267.

© 2026 The Author(s). Published by the Royal Society of Chemistry